

# Radio Meteors

## Study of Sporadic E Occurrence in Europe 2021

Wolfgang Kaufmann<sup>1</sup>

---

The formation of sporadic E layers (Es) over Europe was studied by means of a simple amateur radio station during May to August, 2021. Diurnal solar tides as well as the lunar tide could be clearly identified. Geographical hot spots of preferred Es occurrence were recognized. The reflected radio power showed a distinct Weibull distribution being responsible for a couple of extraordinary high free electron density Es events. The measuring campaign failed to identify a relationship between solar wind induced geomagnetic disturbances and the forming of Es. Also the influence of major meteor showers could not be demonstrated unambiguously.

---

Received 2021 July 19

### 1 Introduction

The term “Sporadic E” (Es) is used for the thin layers of enhanced metallic ionization that form in the E region ionosphere, mostly between about 95 and 120 km. The formation of Es is inextricably linked to meteoroids entering Earth’s atmosphere. Not only the phenomenon itself is worth a study but in terms of radio meteor observation Es also can bias or hamper the recording of meteors. It can produce false positives or suppress the detection of radio reflections off meteors. Hence the study of the Es formation has a practical benefit also. The aim of this paper is to describe the radio observable forming of sporadic E layers (Es) by means of an amateur radio station in the light of scientific insight.

Sporadic E layers can at times become denser than the normal E layer and therefore are an important phenomenon in radio wave propagation up to 150 MHz. Therefore even radio forward scattering observation with the French GRAVES-radar can be affected. The Es occurrence underlies a strong geographical, seasonal and diurnal variation. A comprehensive review gives Haldoupis (2011).

The physics of the mid-latitude sporadic E layer formation is described through the *Windshear Theory*, first proposed and formulated in the early sixties by Whitehead (1961), and Axford (1963). Accordingly the central forces of the forming process of Es are the Earth’s magnetic field, the metallic ion concentration and wind shears in horizontal neutral winds in the mesosphere/lower thermosphere (MLT, corresponding to the ionospheric E region). In the middle atmosphere exist stacked reverse wind flows as zonal as well as meridional wind fields. Between such two reverse horizontal wind flows there exists a layer with a wind shear velocity of null. In case of a westward wind above and an eastward wind below metallic ions in the wind flows are Lorentz-forced by the horizontal component of the magnetic field to drift downwards (upwards) and aggregate in the wind shear null zone. In case of a northward wind above and a southward wind below (in the northern hemisphere) the ions are constrained by the Lorentz

force to gyrate about the inclined magnetic field lines. As a result, the ions finally move in the direction of the magnetic field and therefore converge to the wind shear null to form a layer. Free electrons are then attracted by the positive charge of the compressed ions and move along the magnetic field lines to neutralize this charge (Whitehead, 1997). The resulting high densities of free electrons are responsible for the refraction of radio waves. For the formation of Es-layers zonal winds are significantly more effective than meridional winds.

Vincent (2015) describes the MLT wind dynamics as follows: Zonal mean winds are reaching peak values of approximately 60 to 70 ms<sup>-1</sup> near 70 km and then they reduce in magnitude until they reverse sign at heights between 90 and 100 km. These mean winds are superimposed by planetary waves, atmospheric solar tides and gravity waves. The source regions for all these waves are lower in the atmosphere. As the waves propagate upward their amplitudes grow exponentially to compensate for the decrease in atmospheric density. Consequently, these wave motions often dominate the wind field in the MLT. Especially the atmospheric solar tides with wave periods of a solar day and its sub-harmonics substantially affect the mean MLT-wind flows (Fytterer et al., 2013). They are named diurnal tide (DT, period 24 h), semidiurnal tide (SDT, period 12 h) and terdiurnal tide (TDT, period 8 h) and are responsible for the characteristic diurnal bimodal Es intensity progression.

The metallic ion concentration also is an essential constituent in Es layer forming. Metallic ions have lifetimes from a few days at  $\sim 120$  km to a few hours at  $\sim 95$  km height (MacDougall et al., 2000). Only these persistent ions are able to build up Es layers existing from a few to many hours. These ions originate from incoming meteoroids. The seasonal and geographical variation of the meteoric influx is thought to be responsible for Es occurrence and intensity which is marked by a conspicuous maximum during June–July and a minor peak during December for the northern hemisphere (e.g. Basu et al., 1974). Figure 1 shows the daily meteor counts over middle Europe received by Felix Verbelen at Kampenhout, Belgium, 2020 (personal communication). We find a clear maximum in June/July and a smaller second increase in December.

---

<sup>1</sup>Lindenweg 1e, 31191 Algermissen, Germany. Email: [contact@ars-electromagentica.de](mailto:contact@ars-electromagentica.de).

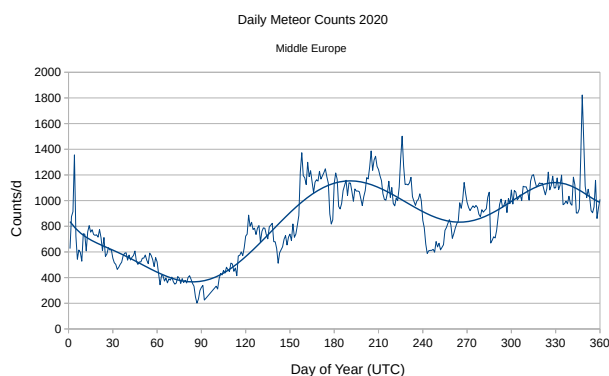


Figure 1 – Daily meteor counts in 2020, recorded in Kampenhout, Belgium, by F. Verbelen using a 2 element Yagi pointing, with an elevation of  $52^\circ$ , to a beacon located near Ieper – distance some 120 km. The beacon is a 2 element crossed yagi pointing to the zenith and beaming a power of 50 Watts (CW) on 49.99 MHz. Data by courtesy of F. Verbelen.

The third important constituent in Es layer forming is the strength of the horizontal field component of magnetic field. It is the key agent responsible for the global Es occurrence distribution. At the two mid-latitude regions of the globe where the horizontal magnetic field is strongly reduced we find the corresponding deep minima in the Es occurrence: one over the south Atlantic in the southern hemisphere and the other over northern America in the northern hemisphere (Arras et. al., 2008).

In this study a CB radio station in the 11 m band was used as hf-beacon as well as receiver. During the minimum of the solar cycle no ionospheric propagation other than via Es will happen. Using the 11 m band enhances the detectability of Es because the amount of radio power being reflected rises with reduced frequency. At least operating a CB-radio is license-free. The digital weak signal mode JS8 is employed. The related en-/decoding software has an automatic reporting function which allows to retrieve reception reports of the own beacon signal all over the world through an internet-accessible database. The logarithmic signal to noise ratio, time and location (given as Maidenhead Grid Locator) of each successful reception are part of these reports. So a pan-European net of CB-radio stations in JS8 mode can be used to observe the occurrence of Es. The number of reports per time unit shall act as a measure of Es occurrence.

## 2 Material and Methods

The 11 m CB-radio station was situated in Algermissen, Northern Germany (Maidenhead locator JO42XG, callsign 13WKA5). A President McKinley transceiver in USB-mode was employed. It was connected to a  $\lambda/4$ -ground-plane antenna (Sirio Signalkeeper) which was mounted 1 m above ground. A computer was connected via a Signalink USB-Interface to the microphone-jack of the transceiver. Digital weak signal mode JS8 (JS8Call v2.2.0 by KN4CRD) was used to transmit heartbeats in normal speed every 6 minutes regularly

between 5 and 20 hours UTC. Former observations with this setup revealed that detecting Es occurrence was largely limited to this time span. However, this period was extended to 24 h in case of the very rare longer lasting propagation conditions. The transceiver was tuned to the international data mode channel 25 (27.245 MHz), the output power was set to 6 W. JS8Call automatically reports all receptions to PSK-reporter<sup>a</sup>. This database was used to get weekly logs of all stations that received 13WKA5 and were received by 13WKA5.

Statistical calculations and plots are done with “PAST” v4.0, Hammer et al. (2001) and the “Free Statistics and Forecasting Software”, Wessa (2021).

The measurements were performed in 2021 from May 1st to August 31th. The solar cycle no. 25 was in its early beginning. Therefore, the solar sun spot number was low and the maximal usable frequency never reached the 11 m band. All propagated signals in the 11 m band were due to Es (any reports from stations via direct or ground wave are excluded).

## 3 Results

The amount of refraction of radio waves that occurs at the Es layer depends on three main factors:

1. the density of free electrons (depending on the metallic ion density),
2. the frequency of the radio wave, and
3. the angle at which the radio waves enters the layer.

In this setup the frequency is fixed. For a given receiving station the angle is also fixed. The radio power received at this station then only depends on the transmitted power and the free electron density in the Es-layer.

Table 1 gives an overview about the number of received reports from European radio stations having decoded successfully JS8-transmissions from 13WKA5 (group 1, G1) as well as reports about stations heard by 13WKA5 (group 2, G2). June and July were the months with the highest number of reports and were used for a couple of analyses. The consistently higher number of G2 reports resulted from stations with a higher HF-output power than the 6 W of the 13WKA5 CB radio station. The higher HF-output compensated for lower free electron densities in the Es-layer resulting in a higher detectability of these stations. For consistent results only the G1-reports were used in the analyses. They are based on constant output-power, constant on-air times and scheduled continuous transmissions of the 13WKA5 CB-station.

The reporting stations were spread all over Europe. Figure 2 shows each station within an azimuthal map centred on the transmitting site in Northern Germany. There are some gaps: the section between  $300^\circ$ – $0^\circ$  covers mostly the North sea and the section between  $60^\circ$ – $120^\circ$  seems to be sparsely populated with JS8-stations.

<sup>a</sup><https://www.pskreporter.info/pskmap.html>

Table 1 – Monthly number of Es related reports 2021. Group 1: number of reports from stations hearing 13WKA5. Group 2: number of stations heard by 13WKA5.

Group Nr.	May	June	July	August
1	637	1563	1735	814
2	1166	2416	2586	1278

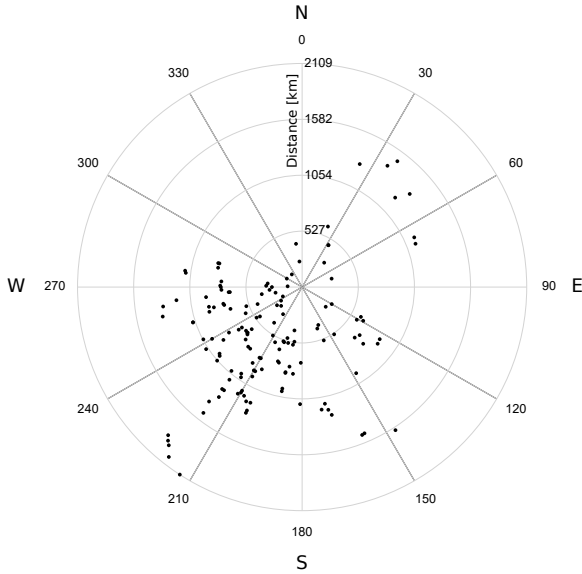


Figure 2 – Azimuthal map of all stations that gave a reception report during the measuring period. The map is centred on the site of the CB radio station 13WKA5 near Hildesheim, Northern Germany.

The number of reported receptions from the single stations were very different. There existed propagation paths that were open almost every day in the June/July-period. On the other hand there were stations, that reported only a small number of receptions. An azimuthal map illustrates the findings showing the number of reports as length of spokes, see Figure 3. Apparently in south-west direction (France, Spain, Portugal) the occurrence of Es was highest followed by north-western directions (southern Sweden, Finland) and last western directions (Ireland, UK). Some bias must be expected by radio stations that are only intermittently on air (e.g. at times of good DX-conditions) thereby missing short Es events.

The graph in Figure 3 could imply that the overall number of reports only resulted from the reporting of a few recurring stations and therefore were not suited as a measure of Es occurrence in general. Hence the number of daily reports were plotted against the number of different locators where the transmissions were received, see Figure 4. The graph reveals a linear relationship with a positive slope. This means the prominent propagation paths in Figure 3 were always part of a set of broadly distributed reception locators.

The distribution of the received logarithmic signal to noise ratio (SNR) of the transmitted signal is depicted in Figure 5. The SNR-span reaches from  $-24$  dB to  $+15$  dB. Thereby, a SNR of  $-24$  dB is the lower thresh-

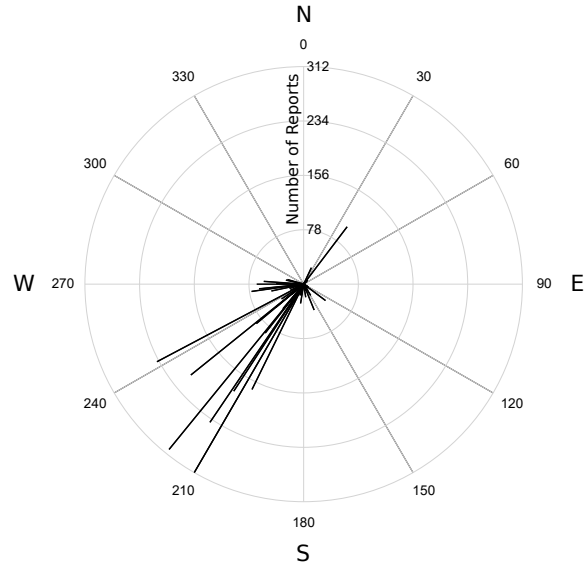


Figure 3 – Azimuthal map of the reporting frequency of radio stations in June/July as length of spokes. The map is centred on the site of the CB radio station 13WKA5 near Hildesheim, Northern Germany.

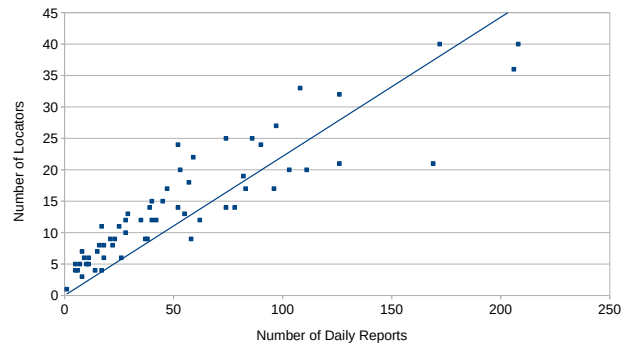


Figure 4 – Number of daily reports from pan-European radio stations in June/July plotted against the number of different locators of reception. A linear function with a correlation coefficient of 0.9 fits the data.

old for a successful JS8 decoding according to the developer of the JS8-mode. The distribution is characterized by a fast rise of reports and a slower decline of reports with increasing SNR. It is best fitted by a Weibull-distribution (shape 2.49, scale 17.5, correlation coefficient 0.99). The elongated tail of the distribution towards higher SNR documents a disproportional higher amount of high free electron density events in the Es-layer compared to a normal distribution.

The daily variation of the SNR per propagation path was found to be very high. Figure 6 shows the progression of the SNR of the transmitted signal during one day received by a French station. This example is typical in its high spread of the SNR within short periods of time and reflects the high dynamics in the MLT. This strong diurnal variability makes the SNR inappropriate for the measurement of Es occurrence rates.

The daily distribution of the number of reports shows a distinct diurnal pattern, see Figure 7. It was

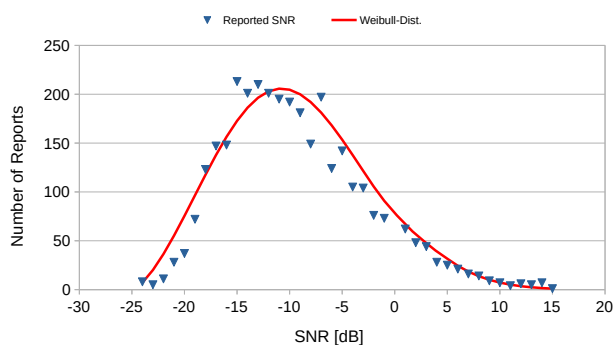


Figure 5 – Frequency distribution of the SNR reported during June/July. A Weibull distribution best fits to the data.

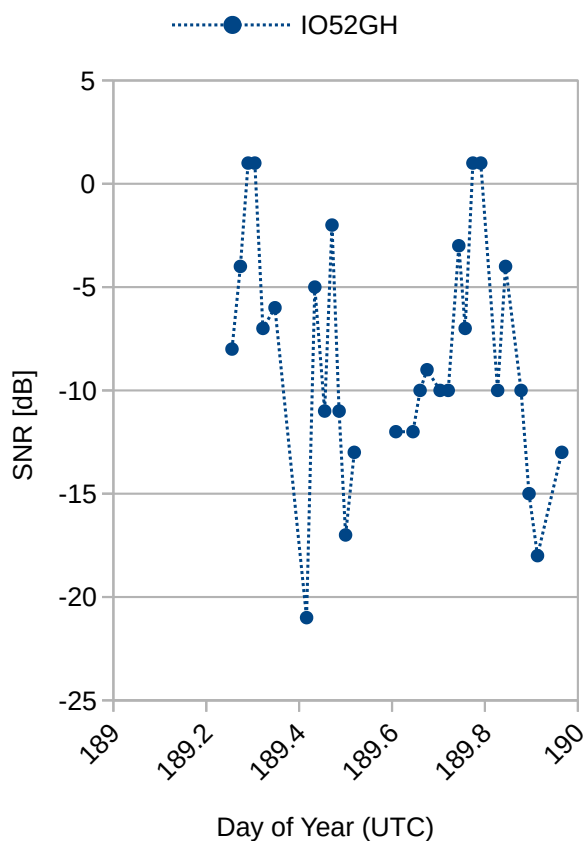


Figure 6 – Variation of the SNR of transmissions from 13WKA5 received by a station in France (Locator IO52GH) on July 8th 2021 UTC.

best fitted with three sinusoids of periods (relative amplitudes) of 23.5 h (1.0), 11.75 h (0.37) and 7.84 h (0.48). This corresponds very well with the periods of the atmospheric solar tides DT, SDT and TDT. It confirms the suitability of the number of reception-reports as a measure of the occurrence rate of Es in principle.

Now we will look at larger scale oscillations of the daily Es occurrence. Figure 8 shows a contour map with the report-density for the period May to August smoothed by a triangular kernel function. The above described diurnal oscillation can be seen well. Interestingly the two daily maxima show differing amplitudes with time. Whereas the Es occurrence in the early evening dominated in May and July the situa-

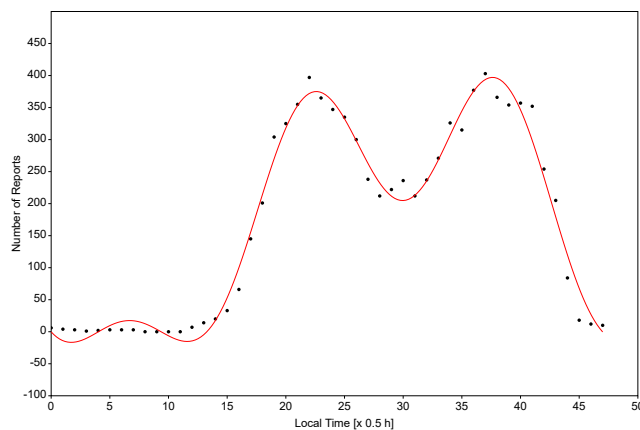


Figure 7 – Total number of reports per half hour local time from June/July. In this analysis the G1- and exceptionally the G2-data were used together to enhance the number of reports to achieve a high correlation coefficient of the sinusoidal fit of 0.98 (The G1-data revealed nearly the same fitting parameters but with a somewhat lower correlation coefficient). Local time is given as CEST.

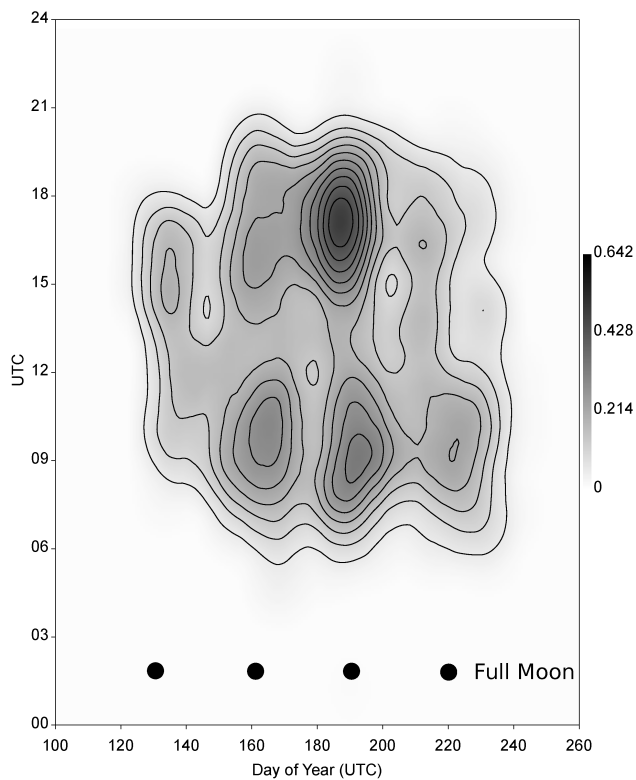


Figure 8 – Contour map of all reports ordered by UTC and day, smoothed by a triangular kernel function (radius = 12.5). The report-density is grey-scale coded. The recording period is May to August. The dates of full moon are indicated.

tion changed in June and August where the Es occurrence dominated in the late morning. Another striking feature is the overall oscillation of the Es occurrence showing periodic maxima coinciding with full moon. A sinusoidal fit revealed a period of 28.83 d which is very close to the 29.53 d of the synodic lunar month.

At least a possible influence of disturbances of the horizontal component of Earth’s magnetic field (Ap-

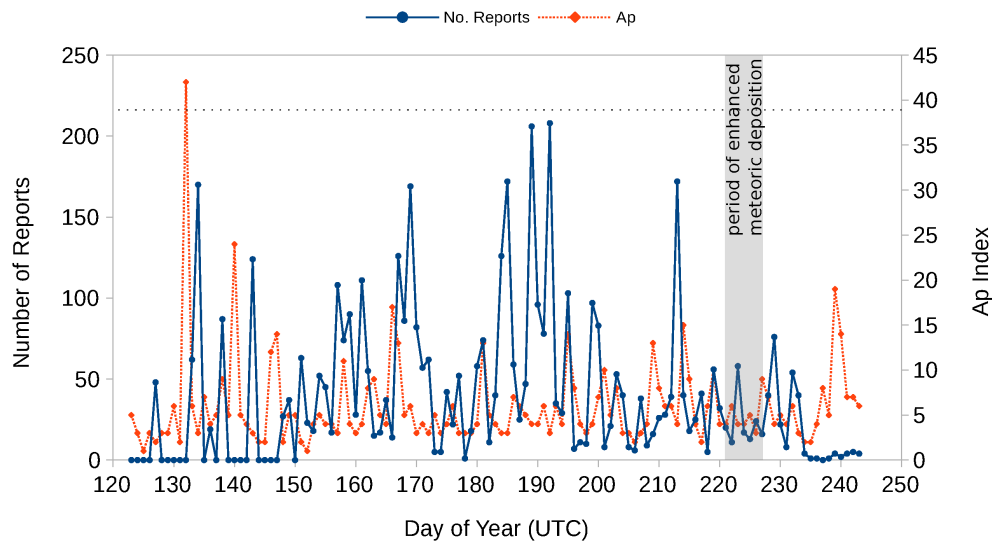


Figure 9 – Number of daily reports in the period May to August and the daily planetary Ap index. The time span of the Perseids as major shower is indicated.

index) and the additional metallic ion deposition from strong meteor showers was considered. Figure 9 shows the daily reports and the planetary Ap index (Matzka et al., 2021). According to NOAA space weather scale<sup>b</sup> a minor geomagnetic storm starts at an Ap-index of 39. Assuming that any influence below this threshold is buried in the highly dynamical processes in the MLT there was only one event at day 132 that exceeds this threshold. At this day no reception was recorded. However, from this single event no general statement can be made.

The same is true with respect to the meteoric influence. Only a strong longer lasting meteor shower may produce a noticeable effect. In the observation period the Perseids was the most prominent meteor shower. It is regarded a major shower in the period August 9th to 15th (gray area in Figure 9) with a maximum zenithal hourly rate (ZHR) of about 100 on August 12th (Rendtel 2014). In this year an additional short but very strong outburst on August 14th between 6 h and 12 h UTC was observed with an ZHR of 210 (Jenniskens & Miskotte, 2021). Looking at Figure 9 the period of enhanced metallic ion deposition may have manifested in a slightly higher number of reports on days 228/229 (August 16th/17th) compared to the previous days. But again from this single observation no general statement can be made.

## 4 Discussion

The results of the measuring campaign correspond well with the findings of ionospheric and climatological research.

1. After considerable averaging the solar and lunar tides clearly could be identified in Es forming (Figures 7, 8). Whereas the solar tides are diurnal atmospheric oscillations caused by the local solar heating of the Earth the roughly monthly lunar tides are understood as a consequence of the gravitational pull of the Moon (Thurman, 1994).

2. Without averaging the Es free electron density is highly variable within minutes to days (Figures 6, 9). It reflects the high dynamical processes in the MLT e.g. driven by shorter scale gravity waves as well as Kelvin-Helmholtz instabilities. Also plasma instabilities have to be regarded.
3. The Es forming is not a uniform process over Europe but there exist preferred locations with a higher than average Es occurrence rate (Figure 4). Locally favoured formation of wind field patterns in the MLT and/or localised electrodynamic processes may be the reason for this.
4. Also the occurrence of highly ionised Es-layers (reflecting radio waves up 150 MHz) is higher than a normal distribution would predict (Figure 5). The noticed Weibull shape often describes a natural wind speed distribution<sup>c</sup>. This could be the reason for the asymmetric occurrence of high free electron density events.
5. The seasonal occurrence of Es is a well known phenomenon that has not been documented here. It is thought that it is a consequence of the seasonal differing overall meteoric deposition of metallic ions. This is in accordance with the measured daily number of meteors over Middle Europe (Figure 1).

A correlation between the Es forming and the disturbance of the geomagnetic field by coronal mass ejections (geomagnetic storms) could not be established because of low number of observations. Also the influence of enhanced short term meteoric metallic ion deposition could not be ascertained. A higher number of observations would be necessary to reliably filter out these effects if they exist anyway.

<sup>b</sup><https://www.swpc.noaa.gov/noaa-scales-explanation>

<sup>c</sup><http://www.reuk.co.uk/wordpress/wind/wind-speed-distribution-weibull/>

## 5 Conclusion

The main determinants of observed Es occurrence can be uncovered by means of a radio amateur. However, only when sophisticated methods and techniques became available, scientific studies could reveal the mechanisms that were able to explain these observations. The “mystery” of Es is much cleared up nowadays but its stochastic behaviour remains. Its occurrence is a question of probability as it is with all complex systems.

## Acknowledgement

The author thanks Felix Verbelen for sharing his radio meteor observation data. This data was highly welcomed, due to the fact it was consistently recorded in the Middle Europe. The author also thanks James DuCharme for double-checking the draft and Jean-Louis Rault for giving valuable advice in his review.

## References

- Arras C., Wickert J., Beyerle G., Heise S., Schmidt T., and Jacobi C. (2008). “A global climatology of ionospheric irregularities derived from GPS radio occultation”. *Geophys Res Lett*, **35:14**, L14809.
- Axford W. I. (1963). “The formation and vertical movement of dense ionized layers in the ionosphere”. *J Geophys Res*, **68:3**, 769–779.
- Basu S., Vesprini R. L., and Aarons J. (1974). “Study of field-aligned ionospheric E-Region irregularities & sporadic E at hf”. *Indian Journal of Radio & Space Physics*, **3**, 70–75.
- Fytterer T., Arras C., and Jacobi C. (2013). “Terrestrial signatures in sporadic E layers at midlatitudes”. *Adv. Radio Sci.*, **11**, 333–339.
- Haldoupis C. (2011). “A tutorial review on sporadic E layers”. In Abdu M. A., Pancheva D., and Bhattacharyya A., editors, *Aeronomy of the Earth’s Atmosphere and Ionosphere*. Springer Science+Business Media B.V., pages 381–394.
- Hammer Å., Harper D. A. T., and Ryan P. D. (2001). “PAST: Paleontological statistics software package for education and data analysis”. *Palaeontologia Electronica*, **4:1**, 9.
- Jenniskens P. and Miskotte K. (2021). “Perseid outburst 2021”. *eMeteorNews*, **6**, 460–461.
- MacDougall J. W., Plane J. M., and Jayachandran P. T. (2000). “Polar cap Sporadic E: part 2, modeling”. *J Atmos Solar-Terr Phys*, **62:13**, 1169–1176.
- Matzka J., Stolle C., Yamazaki Y., Bronkalla O., and Morschhauser A. (2021). “The geomagnetic Kp index and derived indices of geomagnetic activity”. *Space Weather*, **19:5**. <https://doi.org/10.1029/2020SW002641>.
- Rendtel J., editor (2014). *Meteor Shower Workbook 2014*. International Meteor Organisation, Potsdam.
- Thurman H. V. (1994). *Introductory Oceanography, 7th*. Macmillan, New York.
- Vincent R. A. (2015). “The dynamics of the mesosphere and lower thermosphere: a brief review”. *Progress in Earth and Planetary Science*, **2**, 4.
- Wessa P. (2021). “Free Statistics Software, Office for Research Development and Education, version 1.2.1”. <https://www.wessa.net/>.
- Whitehead D. (1997). “Sporadic E–A Mystery Solved? Part 2”. *QST November 1997*, pages 38–42.
- Whitehead J. D. (1961). “The formation of the sporadic E layer in the temperate zones”. *J Atmos Solar-Terr Phys*, **20:1**, 49–58.

---

*Handling Editor:* Jean-Louis Rault